system of hydrogen bonds interconnecting the $[Mn(H_2O)_2(SO_4)_2]^-$ layers mentioned above.

The compound investigated by us seems to be identical with $Mn_2(SO_4)_3.H_2SO_4.nH_2O$ ($n = 4–8$) (Ubbelohde, 1935; Kharabadze, 1963), for which so far only qualitative properties (colour, crystal shape) have been reported.
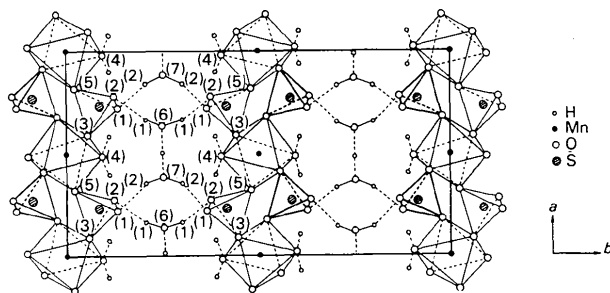

Fig. 1. Projection of the crystal structure of $[H_5O_2][Mn(H_2O)_2(SO_4)_2]$ on (001). The numbering of O and H corresponds to Table 1.

Table 1. *Positional and thermal parameters and their e.s.d.'s*

$$B_{eq} = \tfrac{1}{3}(B_{11} + B_{22} + B_{33}).$$

	x	y	z	$B_{eq}(\text{Å}^2)$
Mn	0·0000	0·0000	0·0000	0·96 (8)
S	0·2325 (8)	0·0858 (5)	0·2835 (2)	1·06 (1)
O(1)	0·2233 (3)	0·3664 (2)	0·4971 (6)	1·68 (4)
O(2)	0·2788 (3)	0·1254 (2)	0·0681 (6)	1·95 (5)
O(3)	0·0873 (3)	0·0564 (2)	0·2446 (5)	1·59 (4)
O(4)	0·0114 (3)	0·5955 (2)	0·2231 (5)	1·68 (4)
O(5)	0·3199 (3)	0·0208 (2)	0·3328 (5)	1·51 (4)
O(6)	0·1349 (6)	0·2500	0·9451 (14)	3·6 (1)
O(7)	0·3831 (6)	0·2500	0·5665 (20)	5·4 (2)

Table 2. *Interatomic distances (Å) and bond angles (°) in the MnO_6, SO_4^{2-} and $H_5O_2^+$ groups with e.s.d.'s in parentheses*

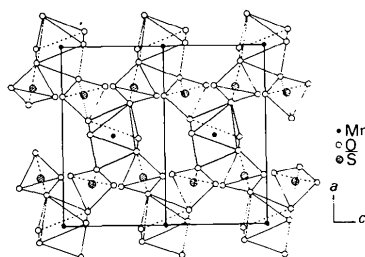|			
Mn–O(3)	2 × 1·885 (2)	O(2)–O(3)	1 × 2·431 (3)
Mn–O(4)	2 × 2·126 (2)	O(2)–O(4)	1 × 2·820 (3)
Mn–O(5)	2 × 1·998 (2)	O(2)–O(5)	1 × 2·424 (3)
S–O(1)	1 × 1·460 (2)	O(2)–O(6)	1 × 2·739 (3)
S–O(2)	1 × 1·453 (2)	O(3)–O(4)	1 × 2·825 (3)
S–O(3)	1 × 1·512 (2)	O(3)–O(4)	1 × 2·858 (3)
S–O(5)	1 × 1·475 (1)	O(3)–O(5)	1 × 2·381 (3)
O(1)–O(2)	1 × 2·416 (3)	O(3)–O(5)	1 × 2·689 (3)
O(1)–O(3)	1 × 2·366 (3)	O(3)–O(5)	1 × 2·804 (3)
O(1)–O(4)	1 × 2·818 (3)	O(4)–O(5)	1 × 2·822 (3)
O(1)–O(4)	1 × 2·922 (3)	O(6)–O(7)	2 × 2·426 (6)
O(1)–O(5)	1 × 2·424 (3)	O(6)–H(1)	2 × 0·945
O(1)–O(7)	2 × 2·643 (3)	O(7)–H(2)	2 × 0·907
O(3)–Mn–O(3)	180·00 (16)	O(1)–S–O(2)	112·06 (13)
O(3)–Mn–O(4)	89·33 (9)	O(1)–S–O(3)	105·49 (12)
O(3)–Mn–O(4)	90·67 (9)	O(1)–S–O(5)	111·34 (13)
O(3)–Mn–O(5)	92·40 (8)	O(2)–S–O(3)	110·14 (13)
O(3)–Mn–O(5)	87·60 (8)	O(2)–S–O(5)	111·73 (13)
O(4)–Mn–O(4)	180·00 (6)	O(3)–S–O(5)	105·70 (12)
O(4)–Mn–O(5)	86·30 (8)		
O(4)–Mn–O(5)	93·70 (8)		
O(5)–Mn–O(5)	180·00 (18)		

Fig. 2. Sheet of composition $[Mn(H_2O)_2(SO_4)_2]^-$ viewed along [010].

References

BROWN, I. D. (1981). *Structure and Bonding in Crystals.* II, pp. 1–30. London: Academic Press.

DOMANGE, L. (1939). *Bull. Soc. Chim. Fr.* **6**, 1452–1459.

ENRAF–NONIUS (1979). *Structure Determination Package.* Enraf–Nonius, Delft.

FRANKE, B. (1887). *J. Prakt. Chem.* **36**, 451–468.

International Tables for X-ray Crystallography (1974). Vol. IV. Birmingham: Kynoch Press.

JANSEN, M., CHANG, F. M. & HOPPE, R. (1982). *Z. Anorg. Allg. Chem.* **490**, 101–110.

JANSEN, M. & HOPPE, R. (1973). *Z. Anorg. Allg. Chem.* **399**, 163–169.

KHARABADZE, N. I. (1963). *Elektrokhim. Margantsa*, **2**, 255–265, 267–278.

UBBELOHDE, A. R. J. (1935). *J. Chem. Soc.* pp. 1605–1607.

The Homologous Series Sb₂S₃.nPbS: Structures of Diantimony Dilead Pentasulphide, Pb₂Sb₂S₅, and the Related Phase Diantimony Ditin Pentasulphide, Sn₂Sb₂S₅

BY P. P. K. SMITH AND B. G. HYDE

Research School of Chemistry, The Australian National University, GPO Box 4, Canberra, ACT 2601, Australia

Abstract. $Pb_2Sb_2S_5$, $M_r = 818·2$, *Pnma*, $a = 19·808$ (5), $b = 4·042$ (2), $c = 11·353$ (4) Å, $V = 909·0$ Å³, $Z = 4$, $F(000) = 1384$; $Sn_2Sb_2S_5$, $M_r = 641·2$, *Pnma*, $a = 19·59$ (3), $b = 3·938$ (3), $c = 11·426$ (3) Å, $V = 881$ Å³, $Z = 4$, $F(000) = 1128$; $\lambda(Cu\,K\alpha_1) = 1·54056$ Å, room temperature. A

homologous series $Sb_2S_3.nPbS$ is obtained by the introduction of layers of thallium iodide ($B33$) type structure into the stibnite structure, parallel to (100) of the latter (*Pnma* setting). For the nth member of the series a sheet of $B33$ n-trigonal-prisms wide is inserted into the stibnite structural motif, giving the approximate lattice parameters $a = 11·31 + 4·22n$, $b = 4·0$, $c = 11·3$ Å, space group *Pnma*. Meneghinite $CuPb_{13}Sb_7S_{24}$, or its Cu-free analogue $Pb_3Sb_2S_6$, corresponds to $n = 3$. $Pb_2Sb_2S_5$ and the isostructural $Sn_2Sb_2S_5$ are shown to represent the $n = 2$ member of this structural series.

Introduction. The system $PbS-Sb_2S_3$ includes at least 17 intermediate minerals and has consequently been the subject of several experimental studies (Garvin, 1973; Hoda & Chang, 1975; Salanci, 1979; Bortnikov, Nekrasov, Mozgova & Tsepin, 1981). As a result of these studies the phase diagram for the system above 673 K is reasonably well established, but the structural relationships between the various phases are as yet incompletely described. Cho & Wuensch (1974) showed that the minerals of the plagionite group constitute a homologous series whose compositions may be expressed by the formula $(3 + 2n)PbS.4Sb_2S_3$ with n taking the values 0 to 3. We describe here a structural relationship between stibnite Sb_2S_3 and meneghinite $CuPb_{13}Sb_7S_{24}$ (or its Cu-free analogue $Pb_3Sb_2S_6$). These compounds are shown to be members of a second homologous series $Sb_2S_3.nPbS$. From this result we predict the structure of $Pb_2Sb_2S_5$ ($n = 2$) and that of the analogous phase $Sn_2Sb_2S_5$.

The series $Sb_2S_3.nPbS$. The structure of meneghinite $CuPb_{13}Sb_7S_{24}$ was determined by Euler & Hellner (1960). Ordering of the Cu atoms leads to a superstructure which need not concern us here; the subcell (Fig. 1) was refined in space group *Pnma* with $a = 24·057$, $b = 4·128$, $c = 11·363$ Å. Copper appears to be an essential constituent of all natural meneghinites, but Wang (1973, 1977) synthesized a Cu-free analogue of meneghinite having the metal-rich formula $4(Pb_{3+x}Sb_2S_6)$ with $0 < x \leq 0·15$ and Salanci (1979) reported a Cu-free meneghinite lying on the $PbS-Sb_2S_3$ join at the composition 26 mol% Sb_2S_3. It is thus apparent that the stoichiometry of the Cu-free meneghinite approximates closely to $Sb_2S_3.3PbS$, copper being incorporated into the natural mineral by means of the substitution of Cu + Pb for Sb. The Cu-free phase has the same space-group symmetry as, and virtually identical lattice parameters to, those of the subcell of natural meneghinite (Table 1).

For the purpose of comparison the structure of stibnite, Sb_2S_3, as determined by Bayliss & Nowacki (1972), is shown in Fig. 2. These authors reported the space group of stibnite to be *Pnma*, but a recent report by Orlyukas & Grigas (1975) suggests that this is only true above a phase transition at 490 K, the low-temperature form having space group $Pn2_1a$. However,

Table 1. *Unit-cell data for members of the series* $Sb_2S_3.nPbS$

	n	a (Å)	b (Å)	c (Å)
Sb_2S_3 (Bayliss & Nowacki, 1972)	0	11·3107	3·8363	11·2285
$PbSb_2S_4$, hypothetical	1	15·53	3·92	11·3
$Pb_2Sb_2S_5$, predicted	2	19·76	4·01	11·3
$Pb_2Sb_2S_5$ (Wang, 1973)*	2	19·80	4·04	11·40
$Pb_2Sb_2S_5$, this study	2	19·808	4·042	11·353
$Pb_3Sb_2S_6$ (Wang, 1977)*	3	23·98	4·10	11·36
$CuPb_{13}Sb_7S_{24}$ (Euler & Hellner, 1960)*†	3	24·057	4·128	11·363

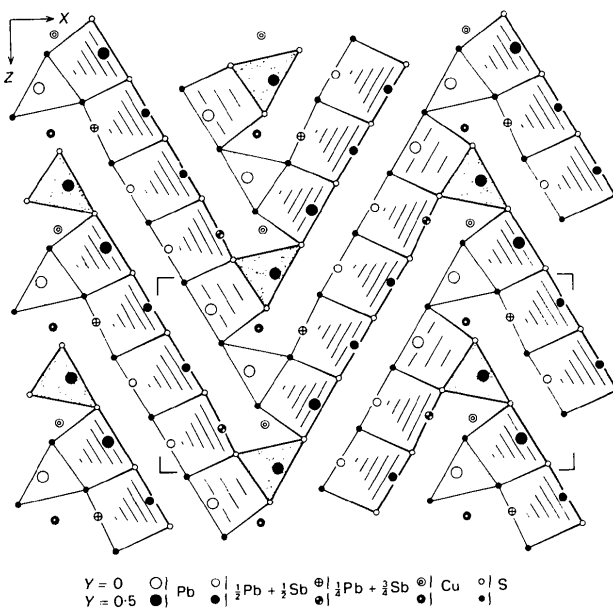* Axes interchanged to correspond to *Pnma* setting.
† Subcell dimensions.

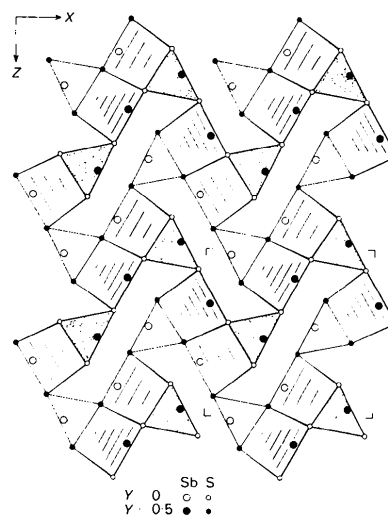Fig. 1. The structure of meneghinite projected on (010).

Fig. 2. The structure of stibnite projected on (010).

any departures from the ideal *Pnma* symmetry are likely to be extremely small and we shall ignore them here.

Stibnite contains two crystallographically distinct SbS₆ trigonal-prism coordination polyhedra: one with its axis perpendicular to the mirror plane ('upright') and one lying parallel to the mirror plane ('horizontal'). The characteristic structural motif of stibnite is formed from two trigonal prisms of each type by edge sharing (Fig. 3a), forming a rod that extends parallel to the *b* axis by means of face sharing between the triangular faces of the upright prisms and edge sharing between the horizontal prisms. In stibnite these rods are linked by edge sharing between upright and horizontal prisms of adjacent rods.

Returning to Fig. 1 we see that the structure of meneghinite may be derived from that of stibnite by inserting three pairs of horizontal trigonal prisms into the stibnite motif, giving the meneghinite structural unit depicted in Fig. 3(d). This is equivalent to the insertion of a slab of thallium iodide type structure (*Strukturbericht* symbol *B*33) parallel to (100) of stibnite. Thus the required Sb₂S₃.3PbS stoichiometry is obtained from Sb₂S₃ by the addition of three formula units of TlI type structure. As anticipated from this structural relationship the *b* and *c* cell parameters of stibnite and meneghinite are similar, but the *a* parameter increases from 11·31 to 23·98 Å in going from stibnite to (Cu-free) meneghinite (Table 1).

This relationship between stibnite ($n = 0$) and meneghinite ($n = 3$) suggests that other structures may be formed by varying the width of the *B*33 slab, corresponding to various values of *n*. Structures produced in this way would also have space-group symmetry *Pnma*, with *b* and *c* lattice parameters close to those of stibnite and an *a* parameter given by $a_n = 11·31 + 4·22n$ Å. Lattice parameters are listed in Table 1 for hypothetical $n = 1$ and $n = 2$ phases, obtained by interpolation from the lattice parameters of stibnite and Cu-free meneghinite; observed lattice parameters for the $n = 2$ phase are given for comparison.

Wang (1973) synthesized a phase of composition Pb₂Sb₂S₅, with probable space group *Pnma* and lattice parameters very close to those that we predict for the $n = 2$ member of the Sb₂S₃.nPbS series (Table 1). Wang (1973) in fact reported that the single-crystal X-ray diffraction patterns obtained from this phase are very similar to those obtained from meneghinite; inspection of the lattice parameters suggests that the structures are related in the manner described above. In a study of the system Sn–Sb–S Wang & Eppelsheimer (1976) synthesized a phase of composition Sn₂Sb₂S₅ with space group *Pnma* or *Pn2₁a* and lattice parameters $a = 19·66$, $b = 3·96$, $c = 11·42$ Å. Single-crystal X-ray patterns indicated that this phase is isostructural with Pb₂Sb₂S₅, but the structure was not determined for either phase.
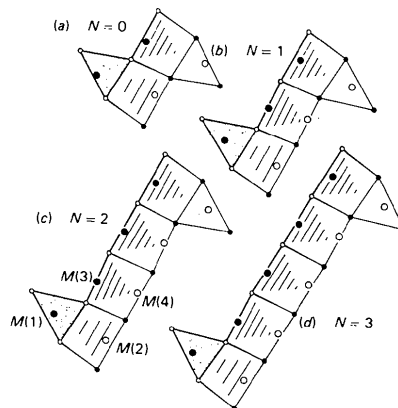

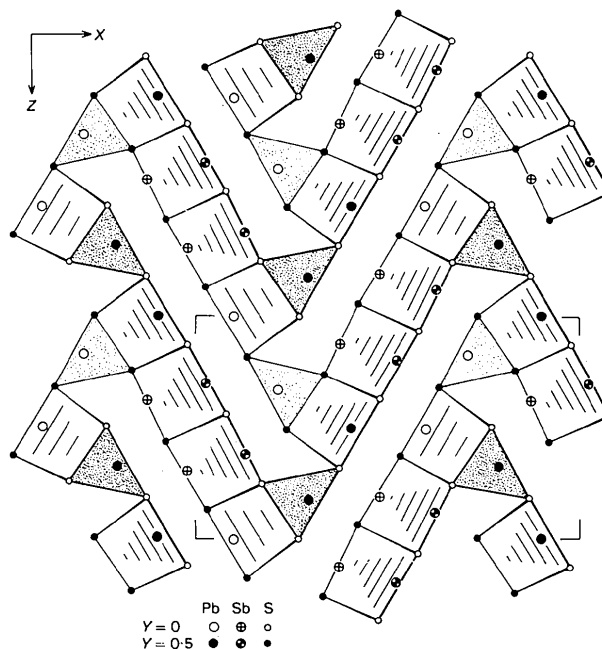Fig. 3. Structural motifs of the first four members of the series Sb₂S₃.nPbS.

Fig. 4. The structure of Pb₂Sb₂S₅ projected on (010).

Table 2. *Atomic coordinates* ($\times 10^3$) *for* Pb₂Sb₂S₅ *and* Sn₂Sb₂S₅

All atoms in sites 4(c) at $x, \frac{1}{4}, z$; $\bar{x}, \frac{3}{4}, \bar{z}$; $(\frac{1}{2}-x), \frac{3}{4}, (\frac{1}{2}+z)$; $(\frac{1}{2}+x), \frac{1}{4}, (\frac{1}{2}-z)$.

	x	z		x	z
M(1) = Pb/Sn	207	171	S(1)	267	491
M(2) = Pb/Sn	100	496	S(2)	869	681
M(3) = Sb	370	376	S(3)	168	744
M(4) = Sb	477	693	S(4)	477	130
			S(5)	080	068

Fig. 4 shows the structure of $Pb_2Sb_2S_5$ and $Sn_2Sb_2S_5$ as predicted for the homologous series $Sb_2S_3.nPbS$; the structure is traced from that of meneghinite with the central $B33$ type (horizontal) trigonal prism eliminated. Atomic coordinates for this structure are given in Table 2. By analogy with the structure of meneghinite we tentatively assign Pb in $Pb_2Sb_2S_5$ to cation sites $M(1)$ and $M(2)$, in the upright prism and the adjacent horizontal prism at the end of the structural motif defined in Fig. 3(c) (i.e. the two sites in the stibnite-like portion of the structure). In meneghinite these are the two largest cation sites, supporting the assignment of Pb to them, although we note that Euler & Hellner's (1960) refinement of meneghinite was relatively insensitive to the cation distribution. The Sn^{II}–S and Sb^{III}–S bond lengths compiled by Jumas, Olivier-Fourcade, Philippot & Maurin (1979) indicate that Sn in $Sn_2Sb_2S_5$ will also prefer the larger $M(1)$ and $M(2)$ sites, but the difference in bond lengths is smaller than is the case for $Pb_2Sb_2S_5$.

Experimental. (1) $Pb_2Sb_2S_5$: Wang (1976) reported that the orthorhombic $Pb_2Sb_2S_5$ phase is not strictly stoichiometric, having a solubility range extending from 34·0 to 36·5 mol% Sb_2S_3 at 863 K. We synthesized this phase from PbS and Sb_2S_3 using charges of composition 34·0 and 35·9 mol% Sb_2S_3.* The reactants were ground together under acetone and heated in evacuated silica tubes for 17 days at 858 K. X-ray powder diffraction patterns were obtained using a Guinier camera and Cu $K\alpha_1$ radiation ($\lambda = 1.54056$ Å) with silicon as an internal standard ($a = 5.4305$ Å). The two compositions gave products with identical powder patterns corresponding to Wang's (1973) $Pb_2Sb_2S_5$. Least-squares refinement of the observed d spacings gives the unit-cell parameters shown in the Abstract.

(2) $Sn_2Sb_2S_5$: This phase may also contain an excess of Sb_2S_3 over that of the ideal formula, having a maximum Sb_2S_3 content of about 39 mol% at 780 K (Wang & Eppelsheimer, 1976). An attempted synthesis at 778 K from a charge containing 36·1 mol% Sb_2S_3 gave the '$Sn_3Sb_2S_6$' phase of Wang & Eppelsheimer (1976), which they reported to have a solubility range from 25 to about 34 mol% Sb_2S_3 at a temperature a few degrees above 773 K. Noting their comment that a trace amount of sulphur will transform the '3:1' phase to the '2:1' phase, we heated the sample, with 0·6 wt% sulphur added, for 10 days at 768 K. This indeed produced the orthorhombic $Pnma$ $Sn_2Sb_2S_5$ phase, indicating that it may lie slightly off the SnS–Sb_2S_3 join. The unit-cell dimensions (Abstract) obtained for this phase are in good agreement with the values reported by Wang & Eppelsheimer (1976).

Relative peak intensities on the Guinier powder diffraction patterns of $Pb_2Sb_2S_5$ and $Sn_2Sb_2S_5$ were measured with a Joyce–Loebl scanning microdensitometer. In Tables 3 and 4* these are compared with intensities calculated for the structure as given in Table 2. The overall agreement is good in both cases and confirms the structural model, although we have made no attempt to refine the structure further. We note here that the calculated intensities for $Sn_2Sb_2S_5$ are insensitive to the M-site cation distribution, since the scattering factors for Sn and Sb are very similar.

Discussion. The powder diffraction data demonstrate that the structure of $Pb_2Sb_2S_5$ is consistent with the model described for the homologous series $Sb_2S_3.nPbS$. The series thus contains the members $n = 0, 2, 3$. No phase of composition $PbSb_2S_4$ ($n = 1$) has been reported, but it is interesting to consider here the mineral twinnite $Pb(Sb,As)_2S_4$ in which the Sb/As ratio varies from 0·80 to 1·92 (Mozgova, Bortnikov, Borodaev & Tzepine, 1982). Jambor (1967) showed that twinnite is the antimonian analogue of scleroclase, $PbAs_2S_4$.

The structure of scleroclase is perhaps best described as an intergrowth of layers of $PbCl_2$ type ($C23$) structure and a rather distorted NaCl type structure (Fig. 5) with Pb in the trigonal prisms of the $PbCl_2$-like layer. However, in Fig. 5 we also present an alternative description of scleroclase in which the $n = 1$ $Sb_2S_3.nPbS$ motif can be identified, albeit in a somewhat sheared form. The linkage of these units in scleroclase clearly differs from that found in the stibnite–meneghinite series, and in fact corresponds to the linkage of the stibnite-like units in α-Gd_2S_3 (Fig. 6). Thus the structure of scleroclase can be derived from that of α-Gd_2S_3 by the insertion of one pair of 'horizontal' trigonal prisms (followed by the shear mentioned above), in a manner analogous to the derivation of $Pb_2Sb_2S_5$ and meneghinite from stibnite.

The $B33$ structure may be derived from $B1$ by a simple shear; the same operation transforms the $CaIrO_3$ structure type to the stibnite type ('unit-cell twinned' $B1$ to twinned $B33$; Hyde, Andersson, Bakker, Plug & O'Keeffe, 1979). In exactly the same way the Cu-free meneghinite structure is derived from the lillianite ($Bi_2S_3.3PbS$) type. In a rather similar way the structure of scleroclase may be related to that of Ru_4Si_3, which belongs to a group of structures derived from $B1$ by glide-reflection unit-cell twinning (Hyde et al., 1979).

---

* Sb_2S_3 was prepared from the elements, both obtained from the American Smelting and Refining Company, New Jersey. PbS and SnS were obtained from Hudson Laboratories, Florida. All starting materials were 99·999% pure.

* These tables have been deposited with the British Library Lending Division as Supplementary Publication No. SUP 38803 (2 pp.). Copies may be obtained through The Executive Secretary, International Union of Crystallography, 5 Abbey Square, Chester CH1 2HU, England.
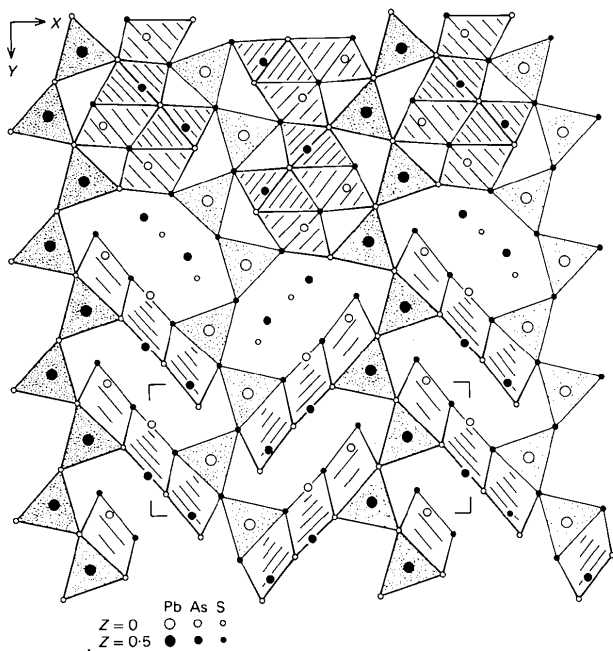
Fig. 5. The structure of scleroclase (Iitaka & Nowacki, 1961) projected on (001). In the upper part of the figure the structure is depicted as alternating layers of PbCl$_2$ type and distorted NaCl type structures. In the lower part of the diagram the structure is depicted as a derivative of the α-Gd$_2$S$_3$ structure type (see Fig. 6).
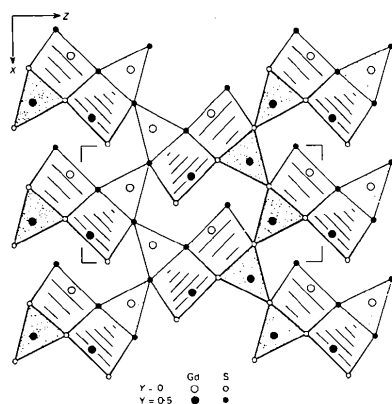

Fig. 6. The structure of α-Gd$_2$S$_3$ projected on (010) (Prewitt & Sleight, 1968).

No compounds have been reported for $n \geq 4$ in the Sb$_2$S$_3$.nPbS system, such compositions being represented by two-phase mixtures of galena with either boulangerite, Cu-free meneghinite, or the uncharacterized phase II (Salanci, 1979). Wang & Eppelsheimer (1976) synthesized compounds corresponding to $n = $ 1,2 and 3 in the system Sb$_2$S$_3$.nSnS, but of these only $n = 2$ belongs to the structural series described in the present paper.

After initial submission of this paper we received the structure determination of Bi$_x$Sb$_{2-x}$Sn$_2$S$_5$ by Kupčik & Wendschuh (1982). The structure of this phase corresponds to that proposed for Pb$_2$Sb$_2$S$_5$ and Sn$_2$Sb$_2$S$_5$ in the present study; the atom positions listed in our Table 1 (determined graphically) are all within 0·3 Å of those reported by Kupčik & Wendschuh (1982). This clearly serves as indirect proof of our structural model, and demonstrates that Pb$_2$Sb$_2$S$_5$ and Sn$_2$Sb$_2$S$_5$ are isostructural with Bi$_x$Sb$_{2-x}$Sn$_2$S$_5$.

References

BAYLISS, P. & NOWACKI, W. (1972). Z. Kristallogr. 135, 308–315.
BORTNIKOV, N. S., NEKRASOV, I. Y., MOZGOVA, N. N. & TSEPIN, A. I. (1981). Neues Jahrb. Mineral. Abh. 143. 37–60.
CHO, S.-A. & WUENSCH, B. J. (1974). Z. Kristallogr. 139, 351–378.
EULER, R. & HELLNER, E. (1960). Z. Kristallogr. 113, 345–372.
GARVIN, P. L. (1973). Neues Jahrb. Mineral. Abh. 118, 235–267.
HODA, S. N. & CHANG, L. L. Y. (1975). Can. Mineral. 13, 388–393.
HYDE, B. G., ANDERSSON, S., BAKKER, M., PLUG, C. M. & O'KEEFFE, M. (1979). Prog. Solid State Chem. 12, 273–327.
IITAKA, Y. & NOWACKI, W. (1961). Acta Cryst. 14, 1291–1292.
JAMBOR, J. L. (1967). Can. Mineral. 9, 191–213.
JUMAS, J.-C., OLIVIER-FOURCADE, J., PHILIPPOT, E. & MAURIN, M. (1979). Rev. Chim. Minér. 16, 48–59.
KUPČIK, V. & WENDSCHUH, M. (1982). Acta Cryst. B38, 3070–3071.
MOZGOVA, N. N., BORTNIKOV, N. S., BORODAEV, Y. S. & TZEPINE, A. I. (1982). Bull. Minéral. 105, 3–10.
ORLYUKAS, A. S. AND GRIGAS, I. P. (1975). Sov. Phys. Crystallogr. 19, 547–548.
PREWITT, C. T. & SLEIGHT, A. W. (1968). Inorg. Chem. 7, 1090–1093.
SALANCI, B. (1979). Neues Jahrb. Mineral. Abh. 135, 315–326.
WANG, N. (1973). Neues Jahrb. Mineral. Monatsh. pp. 79–81.
WANG, N. (1976). Neues Jahrb. Mineral. Abh. 128, 167–175.
WANG, N. (1977). Can. Mineral. 15, 115–116.
WANG, N. & EPPELSHEIMER, D. (1976). Chem. Erde, 35, 179–184.